Integrated network partitioning and DERs allocation for planning of Virtual Microgrids☆

Qigang Wu [a,b], Fei Xue [b,*], Shaofeng Lu [c], Lin Jiang [a], Tao Huang [d], Xiaoliang Wang [a,b], Yiyan Sang [e]

[a] Department of Electrical Engineering and Electronics, The University of Liverpool, Liverpool, L69 3GJ, UK
[b] Department of Electrical and Electronic Engineering, Xi'an Jiaotong - Liverpool University, Suzhou, 215000, China
[c] Shien-Ming Wu School of Intelligent Engineering, Guangzhou International Campus, South China University of Technology, Guangzhou, 511442, China
[d] Politecnico di Torino, Turin, Italy
[e] College of Electrical Engineering, Shanghai University of Electrical Power, Shanghai, 200090, China

ARTICLE INFO

Keywords:
Power system modeling
Power system planning
Complex networks
Microgrids
Renewable energy sources

ABSTRACT

The Virtual Microgrid (VM) method is a solution for addressing challenges in Conventional Distribution Network (CDN), such as power fluctuations or load mismatches, by actively partitioning the CDN into interconnected Microgrid-style VMs. Previous studies have fewer discussions about the mutual interaction between the grid's partition performance and Distributed Energy Resources (DERs) allocation. This paper proposes a new approach for dividing a large power grid into clusters by using the complex network theorem. The approach integrates power flow dynamic, line impedance, generator-load relations and power generator cost-efficiency into a single static weighted adjacency matrix. Meanwhile, a multi-objective Genetic Algorithm (GA) planning structure is also denoted for transforming a CDN to VMs with mutual interaction between partition and DER allocation. The proposed metric is tested in both transmission and distribution networks. The IEEE 118-bus system test shows that even with a higher value of the proposed indicator, there are fewer power exchanges between sub-networks. Meanwhile, in the 69-bus radial system tests, the GA-based co-planning method outperforms previous methods in forming more self-sufficient and more efficient interconnected VMs. An *intermediate* solution is suggested by implementing a trade-off between inter-VM power exchange and the operation cost.

1. Introduction

Requirements from environmental protection have significant impacts on global energy supply policies. For example, recently, China has established a grand target of carbon peak and carbon neutrality. Renewable Energy Source (RES) penetration is expected to have explosive growth in the following decades. However, higher penetration of RES will increase the risk of power fluctuations and load mismatches. Some issues, such as power supply stability, reliability, and quality, should be addressed carefully due to the fact that renewable resources are intermittent. Moreover, electrical power systems control transfer progressively to distributed manners, increasing uncertainty for the power grid's operation [1,2]. Power grid partitioning is becoming a popular topic in transmission and distribution network planning to deal with these challenges. Inspired by the concept of Microgrid, a partitioned distribution network has clearly defined boundaries, and each sub-network could operate as a single controllable entity (i.e. VM) in both grid-connected and islanding operations. Meanwhile, the intermittent distributed RES can be flexibly consumed or balanced locally with reduced impact on neighborhood clustered sub-networks.

The Complex Network (CN) theory provides possible solutions for partitioning a large grid into clusters by considering structural features and the electrical functionality of power grids. Many approaches have been developed for clustering a large network into several sub-nets, such as spectral tree partitioning [3] and the coarsening–partitioning–refinement method [4]. [5] denoted a topological sorting strategy for a directed acyclic graph. It detects the vulnerable cut-sets in the power grid, and the boundary of sub-networks is determined by cut-sets rank. [6,7] developed the original spectral clustering by providing an orthogonal transformation of eigenvectors from spectral clustering.

☆ This work was supported in part by the Research Development Fund (RDF-15-02-14 and RDF-18-01-04) of Xi'an Jiaotong-Liverpool University, in part by the National Natural Science Foundation of China (51877181), and sponsored by Shanghai Sailing Program (22YF1414400).

* Corresponding author.
E-mail address: Fei.xue@xjtlu.edu.cn (F. Xue).

Meanwhile, community structure refers to the composition and inter-relationship of a network community and is one of the most significant features of CN theory [8]. The community detection can be applied to understand the structural characteristics of networks [9]. The *modularity* index in both unweighted and weighted graphs denoted by [10,11] is widely applied in detecting communities in an extensive network. It evaluates the quality of the partitioning of a network into clusters. The fundamental challenge of these topology-based approaches is transforming the power grid into a matrix to represent a graph. However, these works only explore limited aspects (e.g. line impedance) for measuring the importance of each connection between nodes. It may over-simplify the principle of power transmission, including the path of power flows and the power delivery capacity. [12,13] developed the topological adjacency matrix as the combination of reactive power–voltage and real power–voltage sensitivity index. They improved the modularity index with the considerations of reactive power balancing in each sub-networks.

In distribution network planning, with the evolution of CDN into microgrid-style interconnected sub-networks, some papers denoted the concept of VM [14–17]. VM is to partition an existing CDN into several sub-grids with the ability of self-balancing, voltage controllability, energy management, power grid protection, *etc*. Interconnected VMs have similar characteristics to conventional Microgrids, such as Soft Open Point (SOP), island mode operation in an emergency, the ability of self-adequacy, *etc*. Thus, the partitioning of VMs is a crucial problem for the transformation from CDN to interconnected VMs structure. [18] proposed the concept of dynamic Microgrids, which incorporate flexible virtual boundaries. They determined the boundaries of each sub-network dynamically by adjusting the capacity of Distributed Generators (DGs) to maximize the self-adequacy of each partitioned network. Nevertheless, these works discussed the partition strategy from empirical simulations. It is unsuitable for large-scale power grid partitioning as the computation duty may increase rapidly. Meanwhile, they supposed that deployment of DGs is a given condition for VM partitioning; however, the impact of power sources deployment was not considered in the partitioning process.

For addressing the above difficulties, some two-step optimization model for the DGs allocations is suggested in [19–22]. The metric for power grid partition is for minimizing the supply security index related to the power exchange between VMs. The allocation of DERs, including Energy Storage Systems and probabilistic demand, are solved in a subsequent multi-objective model. [20–22] developed VM planning by the concept of complex network theory. They divided the CDN first by the Electrical Coupling Strength (ECS) metric and later allocated DERs to minimize the total operational cost and power exchange between VMs. However, it does not comprehensively evaluate interactions between the quality of power grid partitions and power network economic operations. [23] introduced a co-planning structure for partitioning CDN and allocating DERs simultaneously. They combined the rate of self-adequacy and success indicator of static power flow as a single objective. Nevertheless, it does not provide a clear metric for measuring impacts from the grid's infrastructure. Meanwhile, the number of VMs is determined manually, not from any convinced standards.

In summary, the planning of VMs has two critical tasks, i.e., CDN partitioning and DER allocation. In some works [2,4,7,19,24], DGs have been pre-allocated inside the network. Then they partitioned the CDN by the network's characteristics or the dynamic operating states of generators (and load) only. Alternatively, the partitioning result was determined in advance by structural analysis, and then DERs were allocated within partitioned VMs [20–22]. Different DERs allocations lead to a trade-off between partitioning quality and operational performance. If the objective contains the cost and/or system controllability without measuring the partitioning indicator or *vice versa*, the advantage of VM planning, such as better performance of self-adequacy, cannot be adequately guaranteed. DERs allocation and VMs partitioning have strong mutual interactions during the planning process. However, no paper denotes a simultaneous planning strategy for improving the DERs allocation and quality of partitioning with a clear indicator. Table 1 shows a brief comparison between the former research and our works.

Based on the above discussions, the contributions of this paper can be summarized below:

1. A co-planning method for VMs by concurrent optimization in DERs allocation and CDN partitioning is proposed.
2. Power Functional Strength (PFS) matrix, by integrating static structural, economic and generation-load relations in the power grid is proposed to improve the conventional weighted adjacency matrix.
3. Power Dispatch Modularity (PDM) by PFS in power supply is proposed to evaluate VMs partitioning.
4. An algorithm is introduced to detect optimal VMs partitioning based on PDM.

2. An improved method for power grid partitioning

2.1. The definition of modularity

The modularity index proposed by Girvan and Newman [27] has been widely used for quantitatively measuring the quality of partitioned sub-networks. The potential existence of sub-communities is revealed by comparing the difference between the existent edges in the target network, and the expected number of edges which are placed randomly between nodes. Different from other partition methods, such as the k-means clustering algorithm [28] or searching dynamic boundaries [18] by the Monte-Carlo method, the modularity-based community detection algorithm can search the optimal number of partitioned networks without pre-defining the number of clusters as a constant or heavy computational cost.

Recalling an arbitrary network $N(V, E, W)$, where V represents the set of vertex, $E := \{l(i,j) \subset V \times V\}$ is the set of edges inside the network and W describes the weight of edges. The adjacency matrix A represents a graphical network with an algebraic expression. It is a square matrix of order N_V, which equals the number of nodes in the network. a_{ij} is the ith-row and jth-column element of the adjacency matrix. It indicates the connection and weighting between nodes:

$$a_{ij} = \begin{cases} w_{ij} & l(i,j) \subset E \\ 0 & \text{Otherwise} \end{cases}, \tag{1}$$

where w_{ij} denotes the weight of the connection between node i and j. The modularity index for a weighted (or unweighted) network N is defined as:

$$Q(N) = \frac{1}{2M} \sum_{i \in V, j \in V} [a_{ij} - \frac{k_i k_j}{2M}] \cdot \delta(c_i, c_j), \tag{2}$$

where $M = 1/2 \sum_{ij} a_{ij}$ is the total weight of edges inside the network. $k_i = \sum_j a_{ij}$ and $k_j = \sum_i a_{ij}$ represent the weighted degree value of nodes i and j respectively. c_i (or c_j) is the cluster index where the node i (or j) is allocated. The delta-function $\delta(c_i, c_j)$ yields 1 if $c_i = c_j$ and 0 otherwise. The ordinary modularity index evaluates the performance of partitioned communities from an arbitrary network. However, it over-simplifies the physical characteristics and engineering natures of power grids, such as directional power flow, line impedance, power transmission capacity, *etc*. Therefore, in this study, an enhanced modularity index, Power Dispatch Modularity, is developed to consider these natures comprehensively. This metric is proposed to address two main features while partitioning a conventional distribution network into Virtual Microgrids:

1. To transform the grid's infrastructure factors (e.g. topology, generation capacity, generation cost, *etc*.) into a weighted adjacency matrix.
2. To partition the CDN into several VMs with less interaction between VMs.

Table 1
Comparisons between literature and our works.

Obj.	Solution	Advantage & Disadvantage	Ref.
VM planning	Partitioned-Allocating	Power source deployment is not considered in boundary determination.	[19–22]
	Allocated-Partitioning	Cannot actively enhance functionalities of VM (e.g. self-adequacy).	[2,4,7,19,24]
	Partitioning & Allocating (Single obj.)	Pre-defined the number of VMs; Combines objectives by weighted summation; Not include an indicator for evaluating the partitioned result.	[23]
	This Paper	*Assessing the clustering indicator and cost jointly with flexible number of VMs.*	–
CN expression	One (or two) aspect	Cannot comprehensively consider interactions between factors (e.g. DG cost & capacity, line impedance & connection topology, etc.)	[20–22,25,26]
	This Paper (PFS)	*Combines DGs costs & capacity, line's impedance, capacity & connection topology and power flows dynamic.*	–

Table 2
Approaches of weighted edges and nodes in the power grid.

Objects	Expression of weight	Ref.
Edge	Reactance (or impedance) of the line	[11]
	Equivalent impedance distance	[2]
	Power Transfer Distribution Factors	[31]
	Jacobian of apparent power flow sensitivities	[24]
	Power flow through a line	[2]
	Electrical Coupling Strength (ECS)	[20–22]
	Electrical Functional Strength (EFS)	[26]
Node	Shortest paths through nodes, *betweenness*	[32]
	Load power	[33]

2.2. Modeling the power system as a graph

Based on the complex network theory, a power system can be described as a connected graphical network $N(V, E, W)$. The most straightforward approach to interpret a power grid as a graph is to define the weight of each edge as one equally. It could be considered as a small-world or scale-free network, which is used for discussing structural resilience in the North American power grid [29]. However, the purely topological relations cannot reflect some specific physical features of power system operation, including line impedance or power flow. Meanwhile, electric buses in power grids have different functional roles, such as supplier, consumer, or transmission. The capacity of generation (or demand) is also distinct between buses. The topological expression for network structure cannot present these roles. Therefore, some approaches have been proposed for addressing "electrical" weight of edges and nodes. Table 2 summarizes approaches of weighted edges and nodes inside power grids [25,30].

However, most research focuses on one aspect of edge (or node) weight. [6] denoted a multi-objective optimization for optimizing two weighted metrics: power flows and voltage sensitivity. However, power flow is a dynamic factor. Loads and intermittent DERs output are random and subsequently impact the distribution of power flows. Meanwhile, computational efficiency in [6] is too heavy to integrate into a co-planning structure. The ECS metric proposed in [20–22] combines two isolated features: the equivalent transmission capacity and Thevenin equivalent impedance distance into a single weighted matrix. They allocate two normalized metrics into a two-dimensional coordinator and measure the Euclidean distance between a node and the origin. [26] reinforces the ECS with the consideration of supply–demand relations. They add a direct interaction strength between generator and load into the ECS matrix. This paper will propose a new metric: the PFS. It comprehensively integrates the mutual interaction between the network infrastructure (e.g. topological connection, line impedance, *etc.*), relations between generation-load, and the cost-efficiency of different DERs into an improved adjacency matrix.

2.3. PFS and PDM

This paper aims to upgrade a CDN into an ADN composed of interconnected VMs by partitioning a network and allocating DERs simultaneously. Different combinations of relevant factors of DERs, including installed location and capacity, resource type (e.g., wind, gas, *etc.*), and capital costs, may lead to different power flow distribution through the network. This section describes derivations of PFS and PDM. In addition, the main characteristic of VM is that it can operate under both grid-connected and is-landing modes. Less inter-VM power flows could reduce the influence while switching VM operational modes. Therefore, power flow through boundary lines which connect two VMs is regarded as the interaction factor in the following part.

2.3.1. Power dispatch strength

One distinguishing engineering feature of Virtual Microgrid is to maximize independency and flexibility by minimizing power exchanges between different sub-grids with less impact on daily operational security and efficiency. For a CDN to be upgraded to ADN while its DERs are still underdevelopment, the location and capacity of new DERs may have significant influence on reasonable partitioning. However, this concurrent interaction between partitioning and DERs allocation has never been considered in previous studies about planning of VMs or any self-sufficient autonomous sub-networks. In previous studies, the DERs deployments were either considered as given and fixed conditions, or partitioning was only performed according to structural characteristics of networks but not DERs distribution. Furthermore, even with given network structure and DERs distribution, system operating states may greatly depend on the dispatching principle of operators. Therefore, a reasonable partitioning is expected to be consistent with power dispatching principle. However, up to now, relevant power dispatching factors, especially the economy efficiency in power transmission, have not been considered in the structural partitioning algorithms. Henceforward, in this paper, we propose an improved adjacency matrix: *PDS* which considers DERs distribution, corresponding power supply relations, and the economic aspect of power dispatch.

Power Transfer Distribution Factors (PTDF) is a linear approximation for describing derivations of power flows through a transmission line(s) while injecting power from an arbitrary node. PTDF has been applied to the congestion model or circuit equivalents. It is determined solely by the network topology and transmission line's impedance values. Due to its characteristics of linearity, changes in power flows through the network caused by a unit power injection at node v and withdrawal at node w can be expressed as the difference between vth and wth column of the PTDF matrix [34]:

$$pf_l^{vw} = pf_l^v - pf_l^w, \tag{3}$$

where pf_l^{vw} represents changes of power flows through a particular line l while a unit power exchanges from node v to w. Supposing that there is a generator set $G := \{g(1), \ldots, g(N_G)\}$ and demand set $D := \{d(1), \ldots, d(N_D)\}$ allocated inside the power network $N(V, E, W)$. N_G and N_D are the number of generator and load buses, respectively. If P units of power are injected from a generator g_v and withdrawn by load d_w, power flow variations through the line l is expressed as:

$$\Delta P_l^{g_v d_w}(P) = P \cdot pf_l^{g_v d_w} \qquad g_v \in G, d_w \in D. \tag{4}$$

In addition, the quantity of power delivery between a generator-load pair is constrained by allowable maximum power transmission. The maximum generation capacity constrain is $P_{g_v}^{\max}$, the peak demand

is $P_{d_w}^{\max}$, and the equivalent capacity of transmission pathways in the network is $C_{g_v d_w}$. This equivalent capacity across the network between g_v and d_w is denoted in Eq. (5) for measuring the maximum power flow between two nodes throughout the entire network until the most vulnerable line is crashed. The equivalent transmission capacity is indicated as:

$$C_{g_v d_w} = \min_{l \in E} \left(\left| \frac{P_l^{\max}}{pf_l^{g_v d_w}} \right| \right), \tag{5}$$

where $P_l^{\max}$ is the active power capacity of the particular line l. In conclusion, the power delivery capability between $g-d$ pair is defined as follows:

$$\omega_{g_v d_w} = \min \left(P_{g_v}^{\max}, C_{g_v d_w}, P_{g_v}^{\max} \right). \tag{6}$$

For a particular generator-load pair, the capability to transfer energy from the generator to load through line l is:

$$Pa_l^{g_v d_w} = \Delta P_l^{g_v d_w} \left(\omega_{g_v d_w} \right) = \omega_{g_v d_w} \cdot pf_l^{g_v d_w}. \tag{7}$$

Therefore, electricity will prefer to be transmitted through line l where the value of $Pa_l^{g_v d_w}$ is more significant. Subsequently, the networkwide energy transferring capability through line l, Pa_l is the sum of the absolute value of power transactions from all generator-load pair combinations [35]. It captures the strength of power supply engagement, as reflected in whether more electricity will be potentially transmitted through this line. Hence, the boundary of VMs is preferred to select lines with less value of Pa_l for minimizing the inter-VM power exchange.

$$Pa_l = \sum_{g_v \in G} \sum_{d_w \in D} \left| \omega_{g_v d_w} \cdot pf_l^{g_v d_w} \right|. \tag{8}$$

However, the value of Pa_l cannot reflect the cost-efficiency of different generator-load pairs. Usually, the operator prefers that the system operates under the least-cost condition. The power generation plan is distributed by minimizing costs, including power losses and fuel costs from generators. For this reason, the cost function for different generators will impact dispatches of power flows through lines. Meanwhile, more types of generators, such as wind turbines and gas microturbines, are allocated in modern distribution networks. The cost-efficiency of different types of generators will be distinctive. The system has the best cost performance while operating under the optimal power flow states. However, the real-time nodal load and RES output varies because of the uncertainty of consumer actions or intermittent energy. It is problematic to preserve a fixed generation schedule in partitioning VMs by a Complex Network Approach. Henceforward, we use a simplified Economic Dispatch (ED) under averaged networkwide total demands to estimate the approximate output level for each generator. The objective function of ED is defined as [36]:

$$\text{obj: } \min \sum_{g_v \in G} (a_{g_v} P_{g_v}^2 + b_{g_v} P_{g_v} + c_{g_v}), \tag{9}$$

$$\text{s.t.: } \begin{cases} \sum_{g_v \in G} P_{g_v} = \overline{P_{\text{load}}^{\text{total}}} \\ P_{g_v}^{\min} \le P_{g_v} \le P_{g_v}^{\max} \end{cases}, \tag{10}$$

where a_{g_v}, b_{g_v} and c_{g_v} are the individual fuel cost polynomial coefficient for vth generator located at the bus g_v. The quantity of total power generation is equal to averaged net load $\overline{P_{\text{load}}^{\text{total}}}$ in the designated network. Meanwhile, nodal power output P_{g_v} is constrained by its upper and lower bound $P_{g_v}^{\min}$ and $P_{g_v}^{\max}$, respectively. Then, the estimated duty for different DERs $\hat{P}_{g_v}$ is found by solving the quadratic objectives in Eq. (9) and the estimated output weight of each generator $w_{g_v}^{\text{gen}}$ is:

$$w_{g_v}^{\text{gen}} = \frac{\hat{P}_{g_v}}{P_{\text{load}}^{\text{total}}}. \tag{11}$$

In summary, the following line *PDS* merges the two aspects mentioned above: power transmission capability between generator-load pairs constrained by static parameters, and cost-efficiency of DERs in power dispatch. It is represented as:

$$PDS_{l_{vw}} = \sum_{g_v \in G} \sum_{d_w \in D} w_{g_v}^{\text{gen}} \cdot \left| \omega_{g_v d_w} \cdot pf_l^{g_v d_w} \right|. \tag{12}$$

Furthermore, the N_v-by-N_v PDS matrix is grouped as follows:

$$PDS_{vw} = \begin{cases} PDS_{l_{vw}} & v, w \text{ are connected} \\ 0 & \text{Otherwise} \end{cases}. \tag{13}$$

Meanwhile, to ensure the symmetry of the weighted matrix *PDS*, elements are symmetrical concerning the main diagonal:

$$PDS_{vw} = PDS_{wv}. \tag{14}$$

In conclusion, the pair of generator and demand with lower cost of power supply and better capability in power will have higher ranks inside the network, resulting in a more significant value of *PDS*.

2.3.2. Power functional strength

As discussed in the previous part, the PDS assigns the capability of power dispatch between generator-load pairs with consideration of the economic performance of all generators. However, the prospect mentioned above did not integrate the power losses inside the network, where it cannot be neglected in the distribution network. Similar to ECS and EFS discussed in Table 2, we denote the power functional strength with the integration of *PDS* and the admittance of line:

$$PFS_{vw} = \left| f_N(PDS_{vw}) + j \cdot f_N\left(|Y_{vw}| \right) \right| \tag{15}$$

where $|Y_{vw}|$ represents the magnitude of line admittance between node v and w. Similar to the adjacency matrix, the element PFS_{vw} in the N_v-by-N_v PFS matrix equals zero if node v and w are not connected. If the magnitudes of PDS_{vw} and $|Y_{vw}|$ are significantly different, PFS will be dominated by one aspect. Therefore, the min–max rescaling normalization is applied to eliminate the difference as follows:

$$f_N(x) = \frac{x - \min X}{\max X - \min X}, \tag{16}$$

where x is the element of the non-zero set X.

2.3.3. Power dispatch modularity

Recall Eq. (2), the Power Dispatch Modularity Q_{PD} with improved weighted adjacency matrix PFS is updated as:

$$Q_{PD} = \frac{1}{2M'} \sum_{v,w \in V} \left[PFS_{vw} - \frac{k_v^{PFS} k_w^{PFS}}{2M'} \right] \cdot \delta(c_v, c_w), \tag{17}$$

where $M' = 1/2 \sum_{vw} PFS_{vw}$ is the sum of all PFS in the network and $k_v^{PFS} = \sum_w PFS_{vw}$ and $k_w^{PFS} = \sum_v PFS_{vw}$ are the PFS degree of bus v and w, respectively.

The value of PFS_{vw} denotes the quantity of interactions between two arbitrary nodes. On the other side, if the power network is formed randomly, the expected power functional strength if the weighted edge is placed randomly is, by definition of modularity [27], $k_v^{PFS} k_w^{PFS} / 2M'$. Therefore, larger power dispatch modularity represents higher probabilities of internal power interactions inside a partitioned subnetwork compared with a random network.

2.4. Power grid partitioning algorithm

As mentioned above, a higher value of Q_{PD} represents better quality of partitioning results. Hence, an algorithm is essential for finding the best value of Q_{PD}. The optimal number of partitioned VMs is also decided where Q_{PD} is the maximum. This paper selects the Newman fast algorithm [10] for detecting communities by using power dispatch modularity. The *pseudo*-code of the algorithm is listed in Algorithm 1:

Algorithm 1 Modified Newman fast algorithm for finding max Q_{PD}

Input: Network data, DERs allocation
Output: Partitioned result

Calculate the entire *PFS* matrix;
Separate nodes into clusters and calculate Q^0_{PD};
while Number of clusters $\neq 1$ **do**
  if $\exists\delta(c_i, c_j) = 1$ **then**
    Group two clusters randomly;
  end if
  Calculate the increment of ΔQ_{PD};
  Select the partitioning with maximum ΔQ_{PD};
  Update Q_{PD} according to the result of partitioning;
  Conserve the number of communities;
end while

3. Co-planning for partitioning and DERs allocation

This section proposes an optimal VMs planning scheme with an integrated consideration between partitioning performance features and the economic aspect of DER allocation. Fig. 1 describes the difference between two-stage serial VM-DER planning and our proposed VM-DER co-planning. In previous studies about VMs planning, there are mainly two serial planning methods: partitioning–allocating and allocating–partitioning. The first solution is to partition the network first to identify VMs boundaries according to network structures [20–22]. Subsequently, it optimizes the DERs allocation which is constrained by identified boundaries. However, as illustrated in Fig. 1, with every updating of DER locations and capacities, the network partitioning performance, such as the rate of self-adequacy or power flow sensitivities, would be influenced accordingly. This solution, however, neglects it by assuming the partitioning result is static. The second method plans DERs allocation in the first instance without considering any requirements for self-sufficiency and autonomy of VMs, and then partitions the network into VMs with allocated DERs as fixed conditions [2,4,7,19,24]. However, the DERs allocation in the first step cannot actively adapt to VMs structures and requirements since VMs have not been partitioned at that time. And the partitioning in the second step can only passively adapt to the DERs allocation solution. In reality, mutual interaction between partitioning and DERs allocation exists in daily operations. For these reasons, we propose a multi-objective optimization model in this paper for finding the balance between functional–structural performance and the economic aspect. The objective function maximizes the total modularity of partitioning and minimizes operational costs. A schematic of the co-planning program is illustrated in Fig. 2. In a heuristic optimization process, every time a new DERs allocation scheme is assessed, the network partitioning solution is updated accordingly. Therefore, these two planning targets (i.e. network partitioning and DERs allocation), will be optimized concurrently in an integrated manner.

3.1. Objective function, constraints and optimization algorithm

The multi-objective function of the integrated concurrent planning for VMs is defined as follows:

$$\text{obj:} = \begin{cases} \min f_{daily.}(\alpha) \\ \max\ Q_{PD}(\alpha) \end{cases}. \tag{18}$$

where α is the set of DGs allocation settings. It includes DER's location, type and capacity. Q_{PD} is the value of PDM under the optimal partitioning circumstance. Referring to the definition of PDM, VMs have better performance, because there is less power exchange between inter-VMs while the $Q_{PD}(\alpha)$ increases. $f_{daily.}(\alpha)$ is the cost function of the entire power grid within a given period (e.g. 24 h). It contains the generation cost, installation & replacement cost from DGs, and purchasing cost from the main grid. Meanwhile, a penalty function is added for examining the rate of intermittent renewable source penetration.

3.1.1. Evaluation of cost function

In daily operation, the power dispatch is implemented most economically. The deterministic AC-Optimal Power Flow (AC-OPF) could address the solutions for economic power dispatch within a period. Similar to ED, the objective of AC-OPF is to minimize total generation cost listed in Eq. (19) with additive constraints for power flows:

$$f_{oper} = \min \sum_{g_v \in G} (a_{g_v} P^2_{g_v} + b_{g_v} P_{g_v} + c_{g_v}),$$

$$\text{s.t.:} \begin{cases} \text{E1:} P_i = \sum_{k=1}^{N_{bus}} V_i V_k \left[G_{ik}\cos\theta_{ik} + B_{ik}\sin\theta_{ik}\right] \\ \text{E2:} Q_i = \sum_{k=1}^{N_{bus}} V_i V_k \left[G_{ik}\sin\theta_{ik} + B_{ik}\cos\theta_{ik}\right] \\ \text{I1}: \mathrm{V}_i^{\min} \le |V_i| \le \mathrm{V}_i^{\max} \\ \text{I2}: \mathrm{P}_{g_i}^{\min} \le P_{g_i} \le \mathrm{P}_{g_i}^{\max} \\ \text{I3}: \mathrm{Q}_{g_i}^{\min} \le Q_{g_i} \le \mathrm{Q}_{g_i}^{\max} \\ \text{I4}: S_l \le \mathrm{S}_{l,\max} \end{cases}. \tag{19}$$

The equality constraints Eq. E1 and Eq. E2 represent the active and reactive power balancing for every node i in each time interval t. Eq. I1 describes the limitation for the magnitude of nodal voltage. Eq. I2 and Eq. I3 denote constraints on apparent power P_{g_i}, Q_{g_i} of the generator g_i. Apparent power flow through transmission line l is limited by its rated capacity as shown in Eq. I4. Meanwhile, the structural configuration of CDN is normally radial; the forward–backwards sweep method is used for determining power flows between each node as it has better computational efficiency than the conventional Newton–Raphson method [37]. The radial AC-OPF is implemented by an open-source MATLAB-based simulation package, MATPOWER [38].

The CDN-VMs transformation is performed by installing DERs into the distribution network, leading to extra DER installation and maintenance costs. In this paper, the cost equivalent within a day is proportional to its installed capacity P_n^{cap}:

$$f_{inst} = \sum_{g_v \in G} \left(\mathrm{Co}^{\text{inst.}}_{g_v} \cdot P^{\max}_{g_v}\right) \tag{20}$$

where $\mathrm{Co}^{\text{inst.}}_{g_v}$ is the capital installing & maintaining cost for DERs. Furthermore, for reaching the target of carbon emission, the penetration rate of intermittent renewable sources is also examined. A penalty function is designated for enforcing less RES involved in the VMs. The penalty is in effect while the total installed RES capacity is less than a pre-defined constant $\mathrm{P}^{\min}_{\mathrm{RES}}$.

$$f_{pen} = \begin{cases} 0 & P^{total}_{\mathrm{RES}} > \mathrm{P}^{\min}_{\mathrm{RES}} \\ \mathrm{Co}^{\text{pen}}_{\mathrm{RES}} \left(\mathrm{P}^{\min}_{\mathrm{RES}} - P^{total}_{\mathrm{RES}}\right) & \text{Otherwise} \end{cases}, \tag{21}$$

where $\mathrm{Co}^{\text{pen}}_{\mathrm{RES}}$ and $\mathrm{P}^{\min}_{\mathrm{RES}}$ are constants as capital penalty cost for substandard penetration level and minimum expected capacity of installed RES, respectively. P^{total}_{RES} refers the total amount of actual planned RES in the selected system:

$$P^{total}_{\mathrm{RES}} = \sum_{g_v \in G_{\mathrm{RES}}} P^{\max}_{g_v}, \tag{22}$$

where G_{RES} is the set of intermittent RES generators. In summary, the objective function for assessing the economic aspect within a day is represented as:

$$f^0_{daily} = \sum_T f_{oper} + f_{inst} + f_{pen}. \tag{23}$$

Afterwards, uncertainty variables, such as wind power output or load leveling, are included while assigning the total cost inside the network. Monte-Carlo Simulation (MCS) [39] is a simple and accurate solution for evaluating the uncertainty factors in the power grid operation; therefore, we propose MCS-based AC-Probabilistic-OPF (AC-POPF) as the daily net cost evaluation program in this stage. The

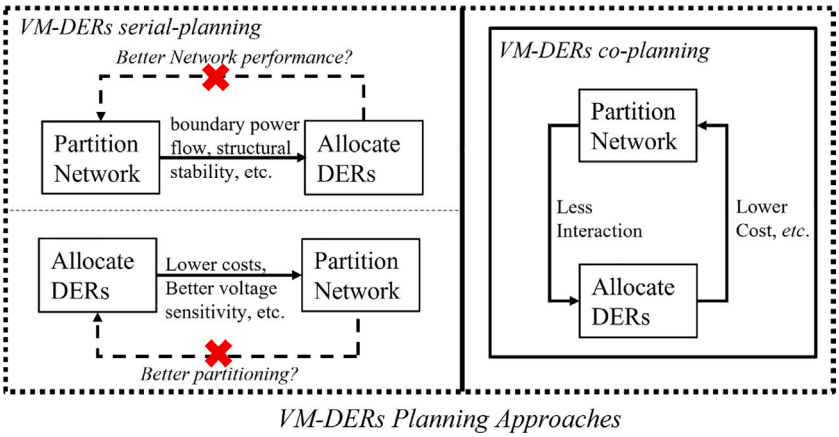

Fig. 1. A comparison between serial planning and co-planning for VM boundaries and DERs allocation. Serial planning strategy cannot revise effects from the secondary aspect.

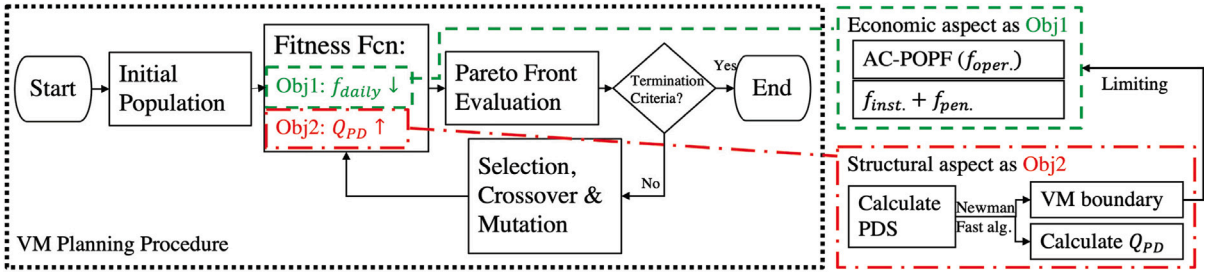

Fig. 2. The schematic of co-planning for VM boundaries and DERs allocation.

probability density function (*pdf*) generates the uncertain load ratio in buses and output from a wind turbine(s). The *pdf* of load between days, months or seasons is different. To reflect the variance of load circumstances, the aforementioned daily cost f_{daily} in Eq. (18) is the sum of cost under different load & wind scenarios with its weight.

$$f_{daily} = \sum_{s} f^{0}_{daily} \cdot w_s, \tag{24}$$

where w_s is the weight factor for different scenarios.

The optimized output for each generator and the total cost in each sample are subsequently calculated by the deterministic radial AC-OPF. The daily cost is assessed by summing costs of all time intervals and the progress is repeated for all samples.

3.1.2. Optimization algorithm

Genetic Algorithm (GA) is emerging as an efficient optimization method that is widely used to solve the non-linear, non-convex optimization [40]. GA has good reliability during the calculation procedure and it can easily collaborate with hybrid optimization approaches [41]. Meanwhile, the optimization problem in this paper includes some non-linear variables; for instance, the capacity for each DER installed in the different bus is discrete as integers. Standard convex relaxation techniques, such as semi-definite programming, may fail to round discrete variables and lead to large errors [42]. Meanwhile, maximizing of modularity indices is NP-hard [8]. Furthermore, unlike the single objective optimization, a trade-off between two objectives occurs until the system's best capabilities are decided in this paper. Compared with weighed sum or ϵ-constraint approximation, the Non-dominated Sorting Genetic Algorithm-II (NSGA-II) have better calculation efficiency and convergence with a single evaluation. Hence, we use a controlled, elitist NSGA-II for finding the Pareto optima between the enhanced modularity Q_{PD} and the cost function f_{cost}. The main work of this stage is for encoding DERs capacity, location & type into chromosomes of GA, defining the fitness function and relevant constraints. The variable is equivalent to a gene, and it constitutes a chromosome. MATLAB Global Optimization Toolbox implements the algorithm.

In practical power engineering, the capacities of DGs are often limited due to investment caps, design targets or socioeconomic resources, et al. Therefore, the multi-objective GA function is firstly restricted by:

$$\sum_{g_v \in G} P^{\max}_{g_v} \le \mathrm{P}^{\max}_{\mathrm{net}}, \tag{25}$$

where $\mathrm{P}^{\max}_{\mathrm{net}}$ is the upper limitation of net DERs capacities. Additionally, DER total capacity in each node is constrained by nodal allowable installation $P^{\max}_{n,\mathrm{total}}$ as:

$$\sum_{g_v @ n} P^{\max}_{g_v} \le P^{\max}_{n,\mathrm{total}}. \tag{26}$$

To guarantee power supply to critical demands while VM(s) operate under the islanding mode, the penetration level of dispatchable DGs is constrained as follows:

$$\frac{\sum_{g_v \in G_{\mathrm{dDG}}} \left(P^{\max}_{g_v} \cdot c_i \right)}{\sum_{d_w \in D} \left(\mathrm{P}^{\mathrm{R}}_{d_w} \cdot c_i \right)} \ge \mathrm{k}_{\mathrm{dDG}}, \tag{27}$$

where G_{dDG} represents the set of dispatchable generators and $\mathrm{k}_{\mathrm{dDG}}$ is the minimum penetration rate of dispatchable generators. $\mathrm{P}^{\mathrm{R}}_{d_w}$ represents the nodal rated demand in bus d_w. c_i denotes the VM index. If the element is located within the area of VM, c_i equals to 1, otherwise 0.

3.2. System modeling

3.2.1. Modeling of generators

Recently, more RES are involved in modern power grid operations. In this paper, we model the uncertainties of wind turbines as the type of non-dispatchable DER and uncertain load demands in the network.

Table 3
Load leveling information in different seasons and day-type.

	S1	S2	S3	S4	S5	S6	S7	S8
Season	Spring		Summer		Autumn		Winter	
Day-type	Wkd	Wknd	Wkd	Wknd	Wkd	Wknd	Wkd	Wknd
w_s	5/28	2/28	5/28	2/28	5/28	2/28	5/28	2/28
μ	0.641	0.551	0.560	0.649	0.624	0.564	0.553	0.678
σ	0.019	0.014	0.016	0.018	0.019	0.015	0.015	0.021

Weibull distribution is utilized as a stochastic model for wind speed distribution [43]. The Probability Distribution Function of the wind speed is as follows:

$$f(v) = \frac{b_{wei}}{a_{wei}} \left(\frac{v}{a_{wei}} \right)^{b_{wei}-1} \exp\left(\left(\frac{v}{a_{wei}} \right)^{b_{wei}} \right), \tag{28}$$

where a_{wei}, b_{wei} are Weibull parameters. The wind turbine rotors extract energy from wind and convert wind energy to electricity by a linked generator. A simplified algebraic relation between wind speed and electrical power is described as follows:

$$P_{wind}(v) = \begin{cases} 0.5 k_{WT} v^3 & v_{ci} < v < v_r \\ P_r & v_r \le v < v_{co} \\ 0 & \text{Otherwise} \end{cases}, \tag{29}$$

where P_{wind} is the power output from a wind turbine generator, v_{ci}, v_{co} and v_r denote the cut-in speed, cut-off speed, and rated wind speed while the wind turbine generates rated power. k_{WT} is a coefficient of the wind turbine. The rated output of the wind turbine is symbolized as a constant P_r. The power output for a wind turbine is stochastic as represented by the *pdf.* of v. However, in performing partitioning according to the definition in Eq. (6), the generation capability P_{g_v} should be a static parameter for generators. The generator's capability for a wind turbine generator under the stage of grid partitioning is selected as its theoretical expected outputs [44].

$$\begin{aligned} P_g^{WT} &= \overline{P^{WT}} = \frac{1}{2} k_{WT} \int_{v_{ci}}^{v_r} v^3 f(v) dv + \int_{v_r}^{v_{co}} P_r dv \\ &\approx \frac{1}{2} k_{WT} a_{wei}^3 \Gamma\left(1 + \frac{3}{b_{wei}}\right) \end{aligned}, \tag{30}$$

where $\Gamma(\cdot)$ is the Gamma function.

In addition, the output of the dispatchable generator is adjustable within the generator's capacity and constrained by Eq. (19).

3.2.2. Modeling of load leveling

Each load follows Gaussian distribution with upper limits L_{up} and lower limits L_{lo} [45]:

$$f_L(lv) = \begin{cases} \frac{1}{\sqrt{2\pi\sigma^2}} \exp\left(-\frac{(lv-\mu)^2}{2\sigma^2} \right) & L_{lo} \le lv \le L_{UP} \\ 0 \quad \text{Otherwise} \end{cases} \tag{31}$$

where lv is the hourly demand leveling. It is the ratio between the real-time demand and its nominal peak load in different nodes. Estimation of μ and σ values are based on the IEEE-RTS [46] system, which provides hourly, daily, and weekly peak load in the percentage of nominal demands. Table 3 summarizes the configuration of parameters in different load scenarios.

4. Case study

In this section, the proposed PDM metric is tested by simulation in the IEEE-118 bus system under different allocations of generators. The second part is the co-planning result for the IEEE-69 bus radial system. The program is run on the following platform: Intel quad-core CPU@3.2 GHz, 8G RAM and MATLAB 2021b. MATPOWER 7.0 implements the AC-PF and AC-OPF. The ED quadratic programming in PDS is solved by MATLAB optimization toolbox.

Table 4
Power plants distribution in 3 testbed systems. Units for $P^r_{g_v}$ & $P^{max}_{g_v}$ are in MW.

Type	Case I	Case II	Case III	$P^r_{g_v}$	$P^{max}_{g_v}$	a_{g_v}	b_{g_v}	c_{g_v}
Wind	10	12	10	308	1000	0.01	5	0
	66	75	60	246.4	800	0.01	5	0
	80	91	79	308	1000	0.01	5	0
Slack	69	77	64	516	805	0.02	20	0
Fuel	12	16	15	85	185	0.12	20	0
	25	34	20	220	320	0.05	20	0
	26	35	23	314	414	0.03	20	0
	31	39	30	7	107	1.43	20	0
	46	57	38	19	119	0.53	20	0
	49	58	39	204	304	0.05	20	0
	54	59	42	48	148	0.21	20	0
	59	63	54	155	255	0.06	20	0
	61	65	55	160	260	0.06	20	0
	65	74	59	391	491	0.03	20	0
	87	94	82	4	104	2.5	20	0
	89	98	87	607	707	0.02	20	0
	100	106	97	252	352	0.04	20	0
	103	107	98	40	140	0.25	20	0
	111	114	110	36	136	0.28	20	0

4.1. Evaluation of PDM performance in IEEE-118 bus system

This part evaluates the performance of the proposed partitioning metric PDM by the IEEE-118 bus system. The target system includes 54 fuel & wind generators, 186 branches and 4242 MW networkwide total peak demand. In the following tests, the configuration of parameters in the load-leveling ratio for all loads is displayed in Table 3 with eight seasonal load scenarios. This part includes three cases for examining the PDM. Case I is the original IEEE-118 bus system with a replacement of 3 fuel generators by wind turbines. For validating the performance of PDM under different power sources allocations, we reshuffle the location of generators in Case II and Case III. Other components, such as network topology or demand distribution, are kept the same in these testbeds. A brief overview of the allocation of generators is listed in Table 4 where 2nd, 3rd and 4th columns represent the location of generators in different cases, respectively. $P^r_{g_v}$ is the nominal quantity of generation analyzed in AC power flow. a_{g_v}, b_{g_v} and c_{g_v} are fuel cost polynomial coefficients for the generator located at the corresponding bus.

All tested cases contain random variables, such as the real-time load-leveling and output of wind turbines. The MCS-based AC-POPF is implemented for addressing the quantity of power flows throughout the network. Factors in Weibull distribution denoted in Eq. (28) are set as $a_{wei} = 10$, $b_{wei} = 2$. The repeat times of MCS in P-OPF is defined as 10 000 times. Furthermore, as introduced in Section 2.3, the boundary power, which equals the quantity of power flows through linkages between partitioned subnetworks, is adopted as the metric for measuring the performance of partitioning. The boundary power flow of a single sub-net $P_{bf}(SN_n)$ is expressed as follows:

$$P_{bf}(SN_n) = \sum_{i \in SN_n} \sum_{j \in V, j \notin SN_n} P_{bf,l}(i,j), \tag{32}$$

where $P_{bf,l}(i,j)$ indicates the quantity of P-OPF power flows through the line between node i inside SN_n and j where outside the cluster. It equals to zero if i and j are not connected directly.

Table 5 lists simulation results from the examined cases. N_{SN} represents the number of clustered sub-nets where the modularity indicator reaches the largest. P^{max}_{bf,c_i} and P^{mean}_{bf,c_i} are the maximum and average value of inter-network power flow, respectively. $P^{max}_{bf,l}$ describes the maximum power flow through a line where connects two sub-nets. For validating the effectiveness of PDM, we involve another four tests with different power grid complex network approaches: topology unweighted adjacency matrix, Equivalent impedance, EFS and power flow matrix introduced in Table 2. The value of power flow matrix is

Table 5
Statistic of boundary power flow under different weights representations in each case study.

	PDM (t = 1.21 s)				Unweighted (t = 1.01 s)				Equivalent Z (t = 10.4 s)				EFS (t = 1.10 s)				Power Flow (t = 1.17 s)			
	N_{SN}	P_{bf,c_i}^{mean}	$P_{bf,l}^{\max}$	$P_{bf,c_i}^{\max}$	N_{SN}	P_{bf,c_i}^{mean}	$P_{bf,l}^{\max}$	$P_{bf,c_i}^{\max}$	N_{SN}	P_{bf,c_i}^{mean}	$P_{bf,l}^{\max}$	$P_{bf,c_i}^{\max}$	N_{SN}	P_{bf,c_i}^{mean}	$P_{bf,l}^{\max}$	$P_{bf,c_i}^{\max}$	N_{SN}	P_{bf,c_i}^{mean}	$P_{bf,l}^{\max}$	$P_{bf,c_i}^{\max}$
Case I	12	193.85	169.83	648.56	11	337.04	226.72	868.06	6	463.70	293.50	606.25	4	338.53	123.55	553.52	7	221.15	142.20	438.09
Case II	10	194.07	122.05	431.32	11	335.75	333.29	725.67	6	629.51	603.77	944.34	5	393.76	235.57	590.19	7	243.49	235.57	552.78
Case III	10	240.56	209.95	563.97	11	446.69	359.20	706.28	6	436.79	584.35	724.48	5	528.88	435.88	879.21	7	251.47	190.78	484.79

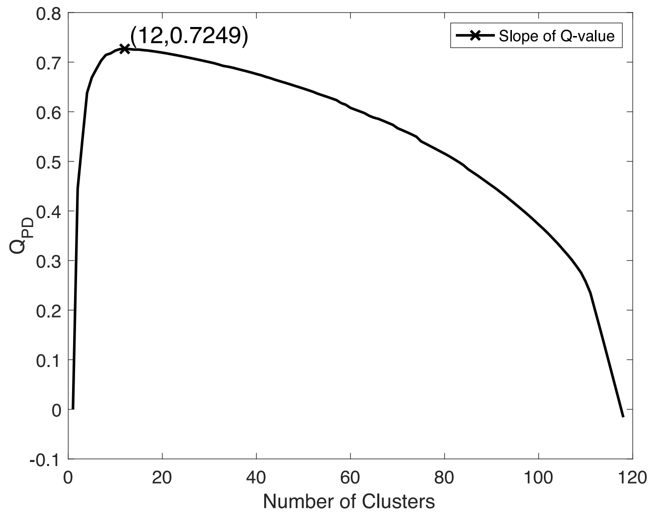

Fig. 3. The partitioned result in Case I by PDM approach.

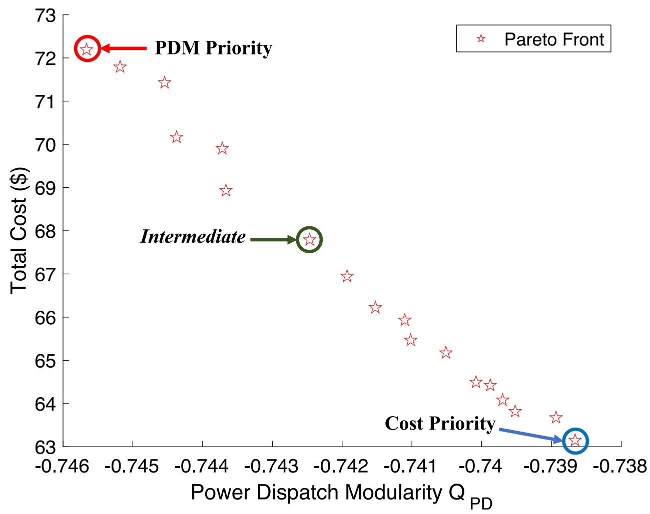

Fig. 4. The Pareto-front of VM-DER co-planning method.

from the system operating under its nominal rated demand and pre-set generation plan listed in the IEEE 118-bus system. These weighted matrixes are processed by the Newman fast community detection described in Algorithm 1, subsequently. For example, Fig. 3 illustrates the trend of PDM in Case I. The modularity indicator Q_{PD} has the largest value of 0.7249 when the 118-bus system is partitioned into 12 clusters. In addition, matrix approaches by pure topology and equivalent Thevenin impedance only depend on the topology connections and line's impedance. It is independent from the allocation of DERs. Therefore, partition results are static in all test cases in unweighted and Thevenin-Z approaches.

The result shows that the proposed PFS approaches have the least averaged sub-nets power exchange P_{bf,c_i}^{mean} in Case I, Case II, and III. The smaller quantity of inter-net power exchanges allows for a smoother

Table 6
Statistic of boundary power flow under *PFS* weights representations in each case study.

	Q_{PD}	$\sum P_{bf,c_i}$	P_{bf,c_i}^{mean}	$P_{bf,c_i}^{\max}$	$P_{bf,l}^{\text{mean}}$	$P_{bf,l}^{\max}$
Case I	0.7249	1163.1	193.85	648.56	39.84	169.83
Case II	0.7332	970.36	194.07	431.32	35.92	122.05
Case III	0.7237	1202.8	240.56	563.97	41.51	209.95

Table 7
System parameter settings in VM-DER co-planning.

$Co_{\text{RES}}^{\text{pen}}$	$P_{\text{RES}}^{\min}$	MC_times	$P_{\text{net}}^{\max}$	$P_{n,\text{total}}^{\max}$
100$/MW	3 MW	1000	10 MW	4 MW

transition from the original operating states to islanding individual operations. In Case II, the max power flow through inter-subnet lines and the maximum and averaged power variation in the cluster of the PDM approach is the smallest in all five metrics. Meanwhile, the averaged computation time for five approaches in three cases is also recorded. Although the proposed PDM solution uses more time than most solutions, no significant difference occurred in all these tested approaches. In conclusion, the PDM representation can provide a better solution for power grid partitioning.

In addition, as denoted in Section 3, the value of Q_{PD} is selected as the indicator of network partitioning performance. The Table 6 records the value of Q_{PD} and power flow metric in all three cases. $\sum P_{bf,c_i}$ represents the total value of inter-subnet power exchange inside the designated system. The inter-subnet power exchanges increase while the system has less value of Q_{PD}. For Case II, it has the best value of Q_{PD} in all three tests, resulting in lower power exchanges in most selected metrics ($\sum P_{bf,c_i}$, $P_{bf,c_i}^{\max}$, $P_{bf,l}^{\text{mean}}$ and $P_{bf,l}^{\max}$). In our proposed model, we prefer to select a system with less inter-cluster power exchange as the better-partitioned scheme. The indicator Q_{PD} can effectively represent the performance of power grid partitioning.

4.2. Implementation of VM-DER co-planning in IEEE-69 bus system

Examinations in the previous section show that the PDM has good performance in power network partitioning. It can effectively reduce interaction between different clusters. Therefore, PDM is selected as the indicator of VM performance. The IEEE-69 radial distribution network is utilized to assess the performance of the VM-DER co-planning procedure. Only one 'main-grid' electricity supplier is addressed in the original system with 68 branches, 48 loads and 3.8 MW total peak demand. A summary of parameter settings denoted in Section 3 is listed in Tables 7 and 8. The mixed-integer, nonlinear-constrained multi-objective function is solved by Multi-Objective Genetic Algorithm (MOGA) with integer variables. Table 9 shows the parameter setting of MOGA in this case, where the Crossover, Mutation and ParetoFrac represent the rate of crossover, the rate of mutation and the fraction of the Pareto Front, respectively.

Fig. 4 illustrates the optimal Pareto front of the VM-DER co-planning method. Eighteen individuals are selected from the Pareto front, where they dominate other individuals by better or lower cost (or both). There is a trade-off between partitioning performance and the total cost introduced in Eq. (18). Two scenarios are selected in the following analysis: the top left with the best modularity and the bottom right

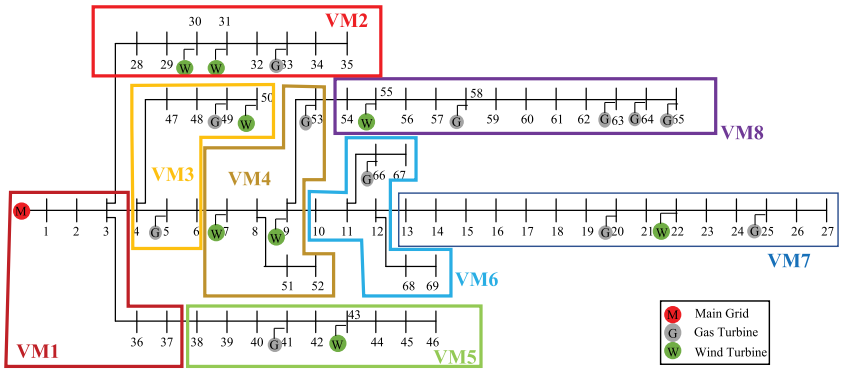

Fig. 5. Schematic of 69-bus system under *Intermediate* condition.

Table 8
DERs parameter settings in VM-DER co-planning.

Type	a_{g_v}	b_{g_v}	c_{g_v}	$Co_g^{inst.}$	k_{dDG}	Min.Unit
Main-grid	0.01	100	0	*N/A*	*N/A*	*N/A*
Wind	0.01	5	0	0.1	*N/A*	0.05 MW
Bio-fuel	0.01	20	0	0.15	50%	0.05 MW

Table 9
Parameter settings in MOGA for 69-bus case.

Pop_{size}	Generation	Crossover	Mutation	ParetoFrac.
150	100(max.) 50(MaxStall)	0.8	0.01	0.3

with the least cost. Meanwhile, VM planned by ECS metric proposed by [20–22] are also compared.

Table 10 compares the daily cost, modularity indicator Q_{PD} and statistics of boundary power flow between four cases. The value of Q_{PD} and cost changes while adjusting DERs allocation. The PDM-Priority and Cost-Priority points are local optima on the Pareto Frontier with biasing on structural integration (evaluated by Q_{PD}) or minimum cost, respectively. In addition, Q_{PD} in [21] is calculated by the definition of modularity with the weighted network approach of the ECS matrix. The objective function of their solution is to minimize total cost under constraints, including zonal dispatchable generator participation and total capacity. The result shows that the proposed PDM-priority VM-DER co-planning has better performance than the Xu's planning strategy, which only considers static network features. The objective (or biased priority) of Cost-Priority and [21] is similar: minimize the total cost during the operation period. Our solution has better cost efficiency than plans in [21]. Boundaries of VMs and their members are flexible in our solutions, leading to a broader search space than the ECS-represented VM plan. Meanwhile, in the average, the maximum and the total quantity of inter-VM power exchanges, our solution still presents more exemplary achievements than the [21] in these aspects.

In addition, compared with the PDM-Priority strategy, Cost-Priority allocation reduces the equivalent daily cost by sacrificing inter-VM interaction, especially the networkwide total inter-VM power exchange $\sum P_{bf,c_i}$. The PDM-priority strategy receives the least networkwide boundaries and averaged inter-VMs power exchange, resulting in VMs' supply–demand relationship being more united internally. Additionally, an *intermediate* strategy is also implemented and listed in the Table 10. In most situations, the planner does not prefer to select plans under extreme conditions. The *intermediate* selection provides a feasible solution which makes a balance between the cost efficiency and network partitioning performance. The schematic of partitioning network by the intermediate method is illustrated in Fig. 5. This plan reduces the inter-VM power exchange efficiently with about $4.64 cost increase more than the minimum-cost plan. In summary, VM-DER

Table 10
Statistic of boundary power flow, operational cost and modularity indicator Q_{PD} in each cases. Unit of power is in MW.

	Min. Cost^M (Cost-priority)	Max. PDM^M (PDM-priority)	*Intermediate*^{M} (Trade-off)	Xu et al. [21]^S (Min. Cost^S)
Cost ($)	63.15	72.39	67.79	64.82
Q_{PD}	0.738	0.746	0.742	0.299[a]
N_{VM}	7	8	8	6
P_{bf,c_i}^{max}	0.217	0.389	0.334	1.982
P_{bf,c_i}^{mean}	0.164	0.079	0.083	0.394
$\sum P_{bf,c_i}$	0.982	0.638	0.662	1.982

^{M} is selected from the Pareto Front of Co-planning solution by MOGA. Min. Cost^M and Max. PDM^M are two extreme points from the Pareto Front.
^{S} is the result of a single-objective function solved by SOGA.
[a]The modularity indicator Q_{PD} in [21] is calculated with its ECS matrix.

Table 11
Comparisons between single-objective GA (SOGA) under extreme conditions (maximize the PDM and minimize cost) and MOGA. PDM-Priority^M and Cost-Priority^M are from co-planning solutions displayed in Table 10.

	Max PDM^S	PDM-Priority^M	Cost-Priority^M	Min Cost^S
Q_{PD}	0.749	0.745	0.738	0.734
Cost	277.61	72.39	63.15	61.34

^{M} is the result selected from the Pareto Front by MOGA
^{S} is the result by SOGA under given objective.

co-planning strategy can address challenges in upgrading CDN into interconnected VMs.

Finally, to ensure the optimality of the multi-objective optimization, we have two more single-objective tests under two extremely conditions: 1. Minimum the total cost and 2. Maximizing the PDM. Results from additional tests are listed in Table 11. The result shows that two extreme scenarios cannot dominate other points on the Pareto front. The case under the Minimum cost objective obtains fewer charges but less PDM, resulting in poorer partitioning performance. Meanwhile, most DG is allocated as bio-fuel DGs in the single-obj. Max. PDM case, resulting in more penalties from insufficient penetration of wind sources denoted in Eq. (21). Therefore, the single-objective solution is unreliable in this case, where it cannot comprehensively consider cost penalties from additional requirements.

5. Conclusion

This paper proposes a new co-planning approach for updating CDN to ADN by interconnected VMs, which also include a new power grid partitioning approach: PFS-based PDM metric Q_{PD}. It visualizes the power grid into a weighted complex network presentation. The power dispatch inside the network is a complicated process, many aspects, such as transmission line capacity or generation cost, should be considered while modeling the network. Compared with other studies,

our approaches comprehensively integrate the power flow dynamic, supply–demand relations, network line impedance and generation cost efficiency into a single static weighted adjacency matrix and processed in subsequent partitioning algorithm. Tests on the 118-bus transmission and 69-bus radial distribution networks show that inter-subnets power exchanges decrease while increasing Q_{PD}, leading to tighter supply–demand relations inside the subnet.

Meanwhile, in the previous study, network partitioning and recourses allocation are treated separately. The serial planning strategy neglects mutual interactions between the partition and operational performance (e.g. cost). We also denote a parallel VM-DER co-planning structure by combining the Q_{PD} and equivalent daily cost into a multi-objective function solved by multi-objective GA. Results from the 69-bus system demonstrate the compromise between cost and Q_{PD} in the Pareto front curve. For balancing these two aspects, we selected an intermediate point as our suggestion for VMs planning. It has a slight increase ($4.64) in cost compared to the minimum cost strategy with much better performance on averaged inter-VMs power exchanges. This paper has denoted an efficient solution for planning the VM with concurrent grid partitioning and resource allocation. However, different control mechanisms and trading strategies from multi-agent VM individuals are also critical in the progress of transformation from the CDN to VM clusters. In future works, coordination between VM-DER planning and islanded individuals' controls, such as enhancing stability or consensus in multi-VMs, can be discussed for transforming the CDN into a multi-VMs structure. The decision-making mechanism of trade games between VM operators can also be developed in later research.

CRediT authorship contribution statement

Qigang Wu: Methodology, Software, Validation, Writing – review & editing. **Fei Xue:** Conceptualization, Methodology, Writing – review & editing, Supervision. **Shaofeng Lu:** Conceptualization, Validation. **Lin Jiang:** Conceptualization, Validation. **Tao Huang:** Conceptualization, Validation. **Xiaoliang Wang:** Validation, Data curation. **Yiyan Sang:** Validation, Data curation.

Declaration of competing interest

The authors declare that they have no known competing financial interests or personal relationships that could have appeared to influence the work reported in this paper.

Data availability

Data will be made available on request.

References

[1] F. Katiraei, R. Iravani, N. Hatziargyriou, A. Dimeas, Microgrids management, IEEE Power Energy Mag. 6 (3) (2008) 54–65.

[2] R.J. Sanchez-Garcia, M. Fennelly, S. Norris, N. Wright, G. Niblo, J. Brodzki, J.W. Bialek, Hierarchical spectral clustering of power grids, IEEE Trans. Power Syst. 29 (5) (2014) 2229–2237.

[3] J.W. Bialek, V. Vahidinasab, Tree-partitioning as an emergency measure to contain cascading line failures, IEEE Trans. Power Syst. 37 (1) (2022) 467–475.

[4] L. Che, X. Zhang, M. Shahidehpour, A. Alabdulwahab, Y. Al-Turki, Optimal planning of loop-based microgrid topology, IEEE Trans. Smart Grid 8 (4) (2017) 1771–1781.

[5] A. Beiranvand, P. Cuffe, A topological sorting approach to identify coherent cut-sets within power grids, IEEE Trans. Power Syst. 35 (1) (2020) 721–730.

[6] Y. Jia, Z. Xu, A direct solution to biobjective partitioning problem in electric power networks, IEEE Trans. Power Syst. 32 (3) (2017) 2481–2483.

[7] I. Tyuryukanov, M. Popov, M.A.M.M. Van Der Meijden, V. Terzija, Discovering clusters in power networks from orthogonal structure of spectral embedding, IEEE Trans. Power Syst. 33 (6) (2018) 6441–6451.

[8] S. Fortunato, Community detection in graphs, Phys. Rep. 486 (3) (2010) 75–174.

[9] X. Li, X. Wu, S. Xu, S. Qing, P.-C. Chang, A novel complex network community detection approach using discrete particle swarm optimization with particle diversity and mutation, Appl. Soft Comput. 81 (2019) 105476.

[10] M.E.J. Newman, Fast algorithm for detecting community structure in networks, Phys. Rev. E 69 (6) (2004).

[11] M.E.J. Newman, Analysis of weighted networks, Phys. Rev. E 70 (5) (2004).

[12] B. Zhao, Z.C. Xu, C. Xu, C.S. Wang, F. Lin, Network partition-based zonal voltage control for distribution networks with distributed PV systems, IEEE Trans. Smart Grid 9 (5) (2018) 4087–4098.

[13] C. Xiao, M. Ding, L. Sun, C.Y. Chung, Network partition-based two-layer optimal scheduling for active distribution networks with multiple stakeholders, IEEE Trans. Ind. Inform. 17 (9) (2021) 5948–5960.

[14] S.A. Arefifar, Y.A.-R.I. Mohamed, T.H.M. El-Fouly, Supply-adequacy-based optimal construction of microgrids in smart distribution systems, IEEE Trans. Smart Grid 3 (3) (2012) 1491–1502.

[15] S.A. Arefifar, Y.A.-R.I. Mohamed, T.H.M. El-Fouly, Comprehensive operational planning framework for self-healing control actions in smart distribution grids, IEEE Trans. Power Syst. 28 (4) (2013) 4192–4200.

[16] T. Lv, Q. Ai, Interactive energy management of networked microgrids-based active distribution system considering large-scale integration of renewable energy resources, Appl. Energy 163 (2016) 408–422.

[17] D.J. Vergados, I. Mamounakis, P. Makris, E. Varvarigos, Prosumer clustering into virtual microgrids for cost reduction in renewable energy trading markets, Sustain. Energy, Grids Netw. 7 (2016) 90–103.

[18] M.E. Nassar, M.M.A. Salama, Adaptive self-adequate microgrids using dynamic boundaries, IEEE Trans. Smart Grid 7 (1) (2016) 105–113.

[19] M. Barani, J. Aghaei, M.A. Akbari, T. Niknam, H. Farahmand, M. Korpas, Optimal partitioning of smart distribution systems into supply-sufficient microgrids, IEEE Trans. Smart Grid 10 (3) (2019) 2523–2533.

[20] X. Xu, F. Xue, S. Lu, H. Zhu, L. Jiang, B. Han, Structural and hierarchical partitioning of virtual microgrids in power distribution network, IEEE Syst. J. 13 (1) (2019) 823–832.

[21] X. Xu, F. Xue, X. Wang, S. Lu, L. Jiang, C. Gao, Upgrading conventional distribution networks by actively planning distributed generation based on virtual microgrids, IEEE Syst. J. 15 (2) (2021) 2607–2618.

[22] M.Z. Oskouei, B. Mohammadi-Ivatloo, O. Erdinc, F.G. Erdinc, Optimal allocation of renewable sources and energy storage systems in partitioned power networks to create supply-sufficient areas, IEEE Trans. Sustain. Energy 12 (2) (2021) 999–1008.

[23] R.A. Osama, A.F. Zobaa, A.Y. Abdelaziz, A planning framework for optimal partitioning of distribution networks into microgrids, IEEE Syst. J. 14 (1) (2020) 916–926.

[24] E. Cotilla-Sanchez, P.D.H. Hines, C. Barrows, S. Blumsack, M. Patel, Multi-attribute partitioning of power networks based on electrical distance, IEEE Trans. Power Syst. 28 (4) (2013) 4979–4987.

[25] P. Cuffe, A. Keane, Visualizing the electrical structure of power systems, IEEE Syst. J. 11 (3) (2017) 1810–1821.

[26] X. Wang, F. Xue, S. Lu, L. Jiang, E. Bompard, M. Masera, Understanding communities from a new functional perspective in power grids, IEEE Syst. J. (2022) 1–12.

[27] M.E.J. Newman, M. Girvan, Finding and evaluating community structure in networks, Phys. Rev. E 69 (2) (2004).

[28] M. Biserica, G. Foggia, E. Chanzy, J.C. Passelergue, Network partition for coordinated control in active distribution networks, in: 2013 IEEE Grenoble Conference, 2013, pp. 1–5.

[29] A.-L. Barabási, R. Albert, Emergence of scaling in random networks, Science 286 (5439) (1999) 509–512.

[30] X. Ma, H. Zhou, Z. Li, On the resilience of modern power systems: A complex network perspective, Renew. Sustain. Energy Rev. 152 (2021) 111646.

[31] R.D. Christie, B.F. Wollenberg, I. Wangensteen, Transmission management in the deregulated environment, Proc. IEEE 88 (2) (2000) 170–195.

[32] E. Bompard, E. Pons, D. Wu, Extended topological metrics for the analysis of power grid vulnerability, IEEE Syst. J. 6 (3) (2012) 481–487.

[33] M.L. Sachtjen, B.A. Carreras, V.E. Lynch, Disturbances in a power transmission system, Phys. Rev. E 61 (5) (2000) 4877–4882.

[34] X. Cheng, T.J. Overbye, PTDF-based power system equivalents, IEEE Trans. Power Syst. 20 (4) (2005) 1868–1876.

[35] A. La Bella, P. Klaus, G. Ferrari-Trecate, R. Scattolini, Supervised model predictive control of large-scale electricity networks via clustering methods, Optim. Control Appl. Methods 43 (1) (2022) 44–64.

[36] D.W. Ross, S. Kim, Dynamic economic dispatch of generation, IEEE Trans. Power Appl. Syst. PAS-99 (6) (1980) 2060–2068.

[37] D. Rajiić, R. Taleski, Two novel methods for radial and weakly meshed network analysis, Electr. Power Syst. Res. 48 (2) (1998) 79–87.

[38] R.D. Zimmerman, C.E. Murillo-Sanchez, R.J. Thomas, MATPOWER: Steady-state operations, planning, and analysis tools for power systems research and education, IEEE Trans. Power Syst. 26 (1) (2011) 12–19.

[39] A. Schellenberg, W. Rosehart, J. Aguado, Cumulant-based probabilistic optimal power flow (P-OPF) with Gaussian and Gamma distributions, IEEE Trans. Power Syst. 20 (2) (2005) 773–781.

[40] M. Ghofrani, A. Arabali, M. Etezadi-Amoli, M.S. Fadali, Energy storage application for performance enhancement of wind integration, IEEE Trans. Power Syst. 28 (4) (2013) 4803–4811.

[41] M. Papadimitrakis, N. Giamarelos, M. Stogiannos, E.N. Zois, N.A.I. Livanos, A. Alexandridis, Metaheuristic search in smart grid: A review with emphasis on planning, scheduling and power flow optimization applications, Renew. Sustain. Energy Rev. 145 (2021).

[42] A. Papalexopoulos, C. Imparato, F. Wu, Large-scale optimal power flow: effects of initialization, decoupling and discretization, IEEE Trans. Power Syst. 4 (2) (1989) 748–759.

[43] D. Villanueva, J.L. Pazos, A. Feijoo, Probabilistic load flow including wind power generation, IEEE Trans. Power Syst. 26 (3) (2011) 1659–1667.

[44] H. Cetinay, F.A. Kuipers, A.N. Guven, Optimal siting and sizing of wind farms, Renew. Energy 101 (2017) 51–58.

[45] K. Zou, A.P. Agalgaonkar, K.M. Muttaqi, S. Perera, Distribution system planning with incorporating DG reactive capability and system uncertainties, IEEE Trans. Sustain. Energy 3 (1) (2012) 112–123.

[46] Probability Methods Subcommittee, IEEE reliability test system, IEEE Trans. Power Appl. Syst. 98 (6) (1979) 2047–2054.